Journal of Molecular Structure 985 (2011) 148–156

Contents lists available at ScienceDirect

Journal of Molecular Structure

journal homepage: www.elsevier.com/locate/molstruc

FT-IR and FT-Raman spectra, vibrational assignments, NBO analysis and DFT calculations of 2-amino-4-chlorobenzonitrile

S. Sudha [a], N. Sundaraganesan [a,*], M. Kurt [b], M. Cinar [c], M. Karabacak [c]

[a] Dept. of Physics (Engg.), Annamalai University, Annamalai Nagar, Chidambaram 608 002, Tamil Nadu, India
[b] Department of Physics, Ahi Evran University, 40100 Kırşehir, Turkey
[c] Department of Physics, Afyon Kocatepe University, 03040 Afyonkarahisar, Turkey

ARTICLE INFO

Article history:
Received 31 August 2010
Received in revised form 24 October 2010
Accepted 25 October 2010
Available online 3 November 2010

Keywords:
FT-IR and FT-Raman
TD-DFT
NBO
HOMO–LUMO
2-Amino-4-chlorobenzonitrile

ABSTRACT

In this work, we report a combined experimental and theoretical study on molecular structure, vibrational spectra and NBO analysis of 2-amino-4-chlorobenzonitrile (2A4CBN). The FT-IR (400–4000 cm^{-1}) and FT-Raman spectra (50–3500 cm^{-1}) of 2A4CBN were recorded. The molecular geometry, harmonic vibrational frequencies and bonding features of 2A4CBN in the ground state have been calculated by using the density functional B3LYP method with 6-311++G (d,p) as higher basis set. The energy and oscillator strength calculated by Time-Dependent Density Functional Theory (TD-DFT) result complements with the experimental findings. The calculated HOMO and LUMO energies show that charge transfer occurs within the molecule. Finally the calculation results were applied to simulate infrared and Raman spectra of the title compound which show good agreement with observed spectra.

1. Introduction

Benzonitrile also called cyanobenzene or phenyl cyanide is an aromatic organic colorless liquid compound with a sweet almond odor. It is air sensitive, eye and skin irritant and widely used as extraction solvent for fatty acids, oils and unsaturated hydrocarbons, removing agent of coloring matters and aromatic alcohols, re-crystallization of steroid, chemical intermediate and solvent for perfumes and pharmaceuticals. Many derivatives of benzonitrile are widely used in industry and medicinal fields. The main products of benzonitrile–benzoic acid are used in medicine as urinary antiseptic in the form of salt and in vapor form for disinfecting bronchial tubes. Benzonitrile derivatives are used in dye industry for making aniline blue and also used for preserving food products [1]. Amino benzonitrile derivatives offer special interest centered in the fast excited state intramolecular charge transfer (ICT) and dual fluorescence [2].

Vibrational spectra of benzonitrile and mono-substituted benzonitriles have been extensively studied [3–8], and also studies have been done on vibrational spectra of some di-substituted benzonitriles [9–11]. Force field calculations have also been made in a few cases [11] using the classical method developed by Wilson to support the vibrational analysis. Mohan et al. [12] reported the laser Raman spectrum of 2-chloro-6-methyl benzonitrile. They carried out assignment of most of the prominent bands in the spectrum based on the assumption that the benzonitrile belongs to the C_s point group.

Recently, Rastogi et al. [13] reported vibrational wavenumbers and several thermodynamic parameters were calculated using *ab* initio quantum chemical methods for the 3,5-difluorobenzonitrile molecule. The results were compared with experimental values with the help of three specific scaling procedures, the observed vibrational wavenumbers were assigned to different normal modes. The rotational spectrum of 3-chlorobenzonitrile and their assignments were analyzed by using *ab* initio calculations [14]. Recently, Fourier transform infrared and Raman spectra of 2-amino-5-chlorobenzonitrile were studied by density functional theory calculations [15].

To the best of our knowledge, neither quantum chemical calculation, nor the vibrational spectra of 2-amino-4-chlorobenzonitrile (2A4CBN) have been reported. Therefore, the present investigation was undertaken to study the vibrational spectra of this molecules completely and to identify the various modes with greater wavenumber accuracy. Density functional theory (DFT) calculation have been performed to support our wavenumber assignments.

2. Experimental

The 2-amino-4-chlorobenzonitrile (2A4CBN) sample was purchased from Sigma–Aldrich Company with a stated purity of 99% and it was used as such without further purification. The sample

* Corresponding author. Mobile: +91 9442068405.
E-mail address: sundaraganesan_n2003@yahoo.co.in (N. Sundaraganesan).

0022-2860/$ - see front matter © 2010 Elsevier B.V. All rights reserved.
doi:10.1016/j.molstruc.2010.10.035

was prepared using a KBr disc technique because of solid state. The FT-IR spectrum of this sample was recorded in the region 400–4000 cm^{-1} on a Perkin Elmer FT-IR BX spectrometer calibrated using polystyrene bands. FT-Raman spectrum of the sample was recorded using 1064 nm line of Nd:YAG laser as excitation wave length in the region 50–4000 cm^{-1} on a Brucker RFS 100/S FT-Raman spectrometer. The detector is a liquid nitrogen cooled Ge detector. Five hundred scans were accumulated at 4 cm^{-1} resolution using a laser power of 100 mW.

3. Computational details

The density functional theory (DFT/B3LYP) at the 6-311++G(d,p) higher basis set level was adopted to calculate the properties of the title molecule 2A4CBN in the present work. All the calculations were performed using Gaussian 03 W program package [16] with the default convergence criteria without any constraint on the geometry [17]. The equilibrium geometry corresponding to the true minimum on the potential energy surfaces (PES) has been obtained by solving self-consistent field equation effectively. The vibrational spectra of the 2A4CBN have been obtained by taking the second derivative of energy, computed analytically. By the use of total energy distribution (TED) using SQM program [18,19] along with available related molecules, the vibrational frequency assignments were made with a high degree of accuracy. The natural bonding orbitals (NBO) calculations [20] were performed using NBO 3.1 program as implemented in the Gaussian 03 W [16] package at the DFT/B3LYP/6-311++G(d,p) level.

4. Prediction of Raman intensities

The Raman activities (SRa) calculated with Gaussian 03 program [16] converted to Raman intensities (IRa) using the following relationship derived from the intensity theory of Raman scattering [21,22].

$$I_i = \frac{f(v_0 - v_i)^4 S_i}{v_i[1 - \exp(-hcv_i/kT)]}$$

where v_0 is the laser exciting wavenumber in cm^{-1} (in this work, we have used the excitation wavenumber v_0 = 9398.5 cm^{-1}, which corresponds to the wavelength of 1064 nm of a Nd:YAG laser), v_i the vibrational wavenumber of the ith normal mode (cm^{-1}), while S_i is the Raman scattering activity of the normal mode v_i. f (is a constant equal to 10^{-12}) is a suitably chosen common normalization factor for all peak intensities. h, k, c and T are Planck, Boltzmann constants, speed of light and temperature in Kelvin, respectively.

5. Results and discussion

5.1. Geometric structure

The optimized geometrical parameters of 2-amino-4-chlorobenzonitrile (2A4CBN) calculated by DFT-B3LYP level with the 6-311++G(d,p) basis set are listed in Table 1, which are in accordance with the atom numbering scheme given in Fig. 1. 2-Amino-4-chlorobenzonitrile is tri-substituted aromatic compound and the substituents are chorine atom, cyanogen group and amino group. The phenyl ring appears a little distorted and angles are slightly out of perfect hexagonal structure. It is due to the fact that substitution of highly electronegative chlorine atom and nitrile group in place of the hydrogen atoms. There is no exact X-ray crystal structure for 2A4CBN, so it is compared with the experimental data of closely related molecule like benzonitrile and 2,6-dichlorobenzonitrile [23,24]. The X-ray data shows that the C—C bond length fall in range 1.371–1.407 Å for benzonitrile and 1.378–1.438 Å for

Table 1
The calculated geometric parameters of 2A4CBN, bond lengths in angstrom (Å) and angles in degrees (°).

Bond lengths (Å)	[a]XRD Benzonitrile (Exp)	[b]XRD 2,6-dichloro benzonitrile (Exp)	B3LYP
C1—C2	1.407(10)		1.397
C1—C6		1.378	1.384
C1—Cl10		1.732	1.754
C2—C3	1.371(11)	1.384	1.385
C2—H7			1.081
C3—C4	1.400(10)	1.403	1.403
C3—H8			1.083
C4—C5			1.418
C4—C11	1.401(14)	1.438	1.424
C5–C6			1.406
C5—N13			1.372
C6—H9			1.083
C11—N12	1.137(14)	1.148	1.158
N13—H14			1.009
N13—H15			1.006
Bond angles (°)			
C2—C1—C6	119.1		122.4
C2—C1—Cl10			119.0
C6—C1—Cl10			118.7
C1—C2—C3	120.5	119.0	118.0
C1—C2—H7			120.7
C3—C2—H7			121.3
C2—C3—C4	119.8	121.3	121.2
C2—C3—H8			120.0
C4—C3—H8			118.8
C3—C4—C5	120.3		120.3
C3—C4—C11	119.9		120.8
C5—C4—C11			119.0
C4—C5—C6			118.2
C4—C5—N13			121.1
C6—C5—N13			120.7
C1—C6—C5			120.0
C1—C6—H9			120.1
C5—C6—H9			119.9
C5—N13—H14			119.0
C5—N13—H15			118.8
H14—N13—H15			115.9

[a,b] Taken from Refs. [23,24].

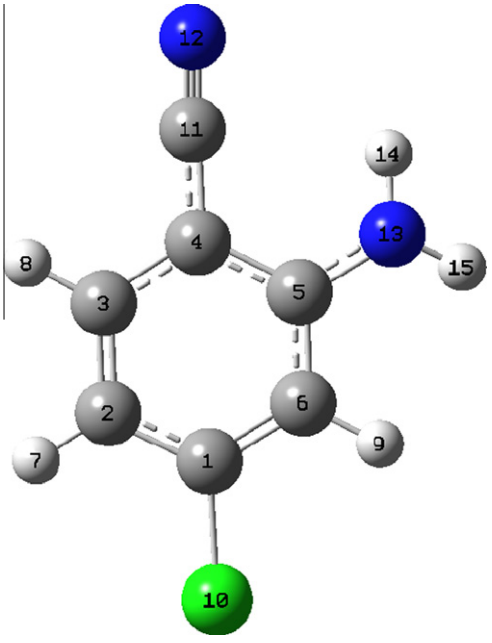

Fig. 1. Molecular structure and atom numbering scheme adopted in this study for 2-amino-4-chlorobenzonitrile.

2,6-dichlorobenzonitrile. Krishnakumar and Dheivamalar [15] calculated the same C—C bond length in the range 1.370–1.432 Å for 2-amino-5-chlorobenzonitrile by B3LYP/6-311++G** method. In our title molecule, the optimized C—C bond length in 2A4CBN fall in the range 1.384–1.424 Å by B3LYP/6-311++G(d,p) method. These values show that our calculation results are more consistent with the experimental data. For the title compound, the bond length of the cyanogen group (C≡N) predicted by B3LYP/6-311++G(d,p) method is 1.158 Å and it shows excellent agreement with the experimental data of 1.137 Å for benzonitrile and 1.148 Å for 2,6-dichlorobenzonitrile and show small deviation of 0.006 Å, which is shorter than the C—N single bond length of 1.372 Å. The N—H and C—H bond lengths and bond angles are also very similar with that of the 2-amino-5-chlorobenzonitrile molecule reported by Krishnakumar and Dheivamalar [15] The ring C—C—C bond angles, C1—C2—C3 and C4—C5—C6 are slightly smaller than 120° and C2—C1—C6, C2—C3—C4 and C3—C4—C5 are slightly larger than 120°.

5.2. Vibrational assignments

The optimized structural parameters were used to compute the vibrational frequencies of 2A4CBN at the DFT, B3LYP/6-311++G(d,p) level of calculation. The 39 normal modes of the title compound are distributed as 27A′ + 12A″ in agreement with C_s symmetry and the proposed vibrational mode assignments are collected in Table 2. The experimental and theoretical FT-IR and FT-Raman spectra are shown in Figs. 2 and 3. The simulated IR and Raman spectra have been plotted using pure Lorentzian band shapes with band width of Full Width and Half Maximum of 10 cm^{-1}. All the vibrations are active both in IR and Raman. The total energy distribution (TED) for each normal mode among the symmetry coordinates of the molecules was calculated. A complete assignment of the fundamentals was proposed based on the calculated TED values, infrared and Raman intensities. The observed FT-IR and FT-Raman frequencies for various modes of vibrations are presented in same table for comparison reason. Reduction in the computed harmonic vibrations, though basis set sensitive are only marginal as observed in the DFT values using 6-311++G(d,p). Any way not withstanding the level of calculations, it is customary to scale down the calculated harmonic frequencies in order to improve the agreement with the experiment. Due to some systematic errors, however, some sort of empirical correction of the force field is required to obtain an acceptable agreement (in the order 15–20 cm^{-1}) of observed and calculated frequencies. In

Table 2
Comparison of the calculated and experimental vibrational spectra and proposal assignments of 2A4ClBN.

Species	Experimental			B3LYP/6-311++G(d,p)				TED (⩾10%)
	Mode nos.	FT-IR	FT-Raman	Unscaled	Scaled	[a]I_{IR}	[b]I_{Ra}	Assignments
A′	1	3456s		3703	3487	42.45	1.9	*v*asym NH_2 (100)
A′	2	3369vs		3588	3378	66.33	7.22	*v*sym NH_2 (100)
A′	3			3218	3085	0.02	8.19	*v*CH (100)
A′	4	3087w	3089m	3194	3062	0.44	7.07	*v*CH (100)
A′	5		3070w	3192	3060	2.05	2.66	*v*CH (100)
		2926vw					100	Overtone/combination
		2763vw					5.45	Overtone/combination
A′	6	2213vs	2215vs	2314	2227	87.59	25.46	*v*C≡N (90) + *v*CC (10)
A′	7	1642vs	1654w	1664	1590	226.81	11.1	*ρ*NH_2 (88)
A′	8	1609s	1610w	1635	1582	122.37	3.78	*v*CC (62) + *ρ*NH_2 (12) + *β*CH (11)
A′	9	1565ms	1559w	1590	1539	60.07	0.58	*v*CC (74) + *β*CNH (10)
A′	10	1487w	1487m	1515	1466	73.42	13.25	*β*CH (53) + *v*CC (32)
A′	11	1435w		1458	1411	48.74	0.59	*v*CC (35) + *v*C—NH_2 (28) + *β*CH(17)
A′	12	1330s	1330w	1349	1328	7.37	8.06	Ring deformation (*v*CC) (83)
A′	13	1281m		1304	1261	8.47	21.02	*β*CH (80)
A′	14	1266ms	1265m	1287	1241	65.45	6.6	*v*CC (44) + *v*C—NH_2 (21) + *β*CH (18)
A′	15	1186w	1189w	1215	1184	5.11	12.61	*v*C—C≡N (37) + *β*CCC (25) + *β*CH (15)
A′	16	1140w	1139w	1156	1118	2.57	4.87	*β*CH (50) + *r*NH_2 (16) + *β*CC (12)
A′	17	1097w	1094w	1111	1075	25.87	1.9	*v*CC (41) + *β*CH (27) + *r*NH_2 (11)
A′	18	1052w	1050w	1059	1012	11.66	7.22	*r*NH_2 (41) + *v*CC (35)
A″	19	936w		962	943	0.71	0.07	*γ*CH (90)
A′	20	919m		924	914	73.12	0.89	*v*CCl (26) + *β*CCC (43) + *v*C—NH_2 (15)
A″	21			858	841	20.97	0.23	*γ*CH (87)
A″	22	786w		810	794	32.62	0.66	*γ*CH (85)
A″	23		737s	749	726	0.44	11.25	*τ*CCCH (33) + *τ*CCCC (29)
A″	24	715ms		746	736	0.51	22.34	Ring breathing (65)
A′	25	620w	622m	627	608	3.38	3.34	*β*CC≡N (49) + *β*CCC (33)
A′	26			625	615	3.85	2.37	*ω*NH_2 (30) + *v*CCl (22) + *β*CC≡N (21)
A″	27	601w		618	599	5.70	0.89	*τ*CCCC (35) + *τ*CCCH (28) + *τ*CCCN (10)
A″	28	525w		536	519	6.87	3.37	*τ*CCC≡N(62) + *τ*CCCH (10)
A′	29	508w	507m	515	508	3.88	13.20	Ring breathing (41) + *β*CC≡N (20) + *v*CCl (22)
A″	30	421w		439	425	1.22	0.78	*τ*CCCC (38) + *τ*CCCH (23) + *τ*CCNH (17)
A′	31	417w	420w	420	401	4.47	2.49	*r*NH_2 (51) + *β*CCCl (20) + *β*CC≡N (12)
A″	32			400	393	30.71	1.23	*t*NH_2 (84)
A′	33		353m	349	343	1.91	25.11	*v*CCl (35) + *β*CCC (30)
A″	34			329	323	241.03	2.31	*ω*NH_2 (95)
A′	35		255w	250	246	1.27	10.44	*β*CCCl (64) + *r*NH_2 (20)
A″	36		218m	243	235	2.53	0.32	*τ*CCCN (35) + *τ*CCCCl (24) + *τ*CCCC (18)
A″	37			200	194	2.59	3.08	*τ*CCC—NH_2 (40) + *τ*CCCCl (26) + *τ*CCCC (20)
A′	38			137	135	7.08	39.39	*r*C—C≡N (44) + *β*CCC (40)
A″	39		89vs	85	82	3.26	15.27	*τ*CCCC (36) + *τ*CCCN(20) + *τ*CCCCl (18)

v – Stretching; *β* – in-plane-bending; *γ* – out-of-plane bending; *ρ* – scissoring; *ω* – wagging; *r* – rocking; *t* – twisting; *τ* – torsion.
[a] I_{IR} – IR intensity (K $mmol^{-1}$).
[b] I_{Ra} – Raman intensity (Arb. units) (intensity normalized to 100%).

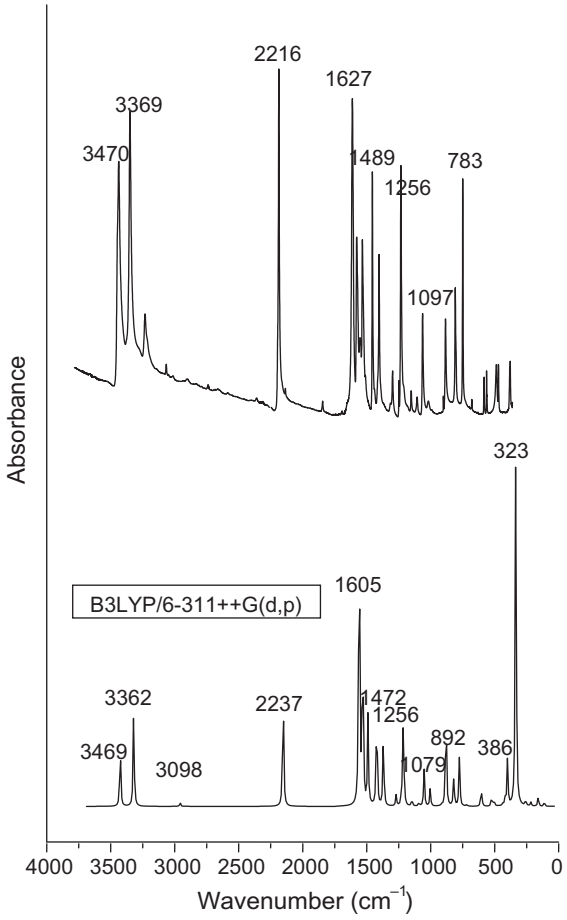

Fig. 2. Comparison of experimental and theoretical FT-IR spectra of 2-amino-4-chlorobenzonitrile.

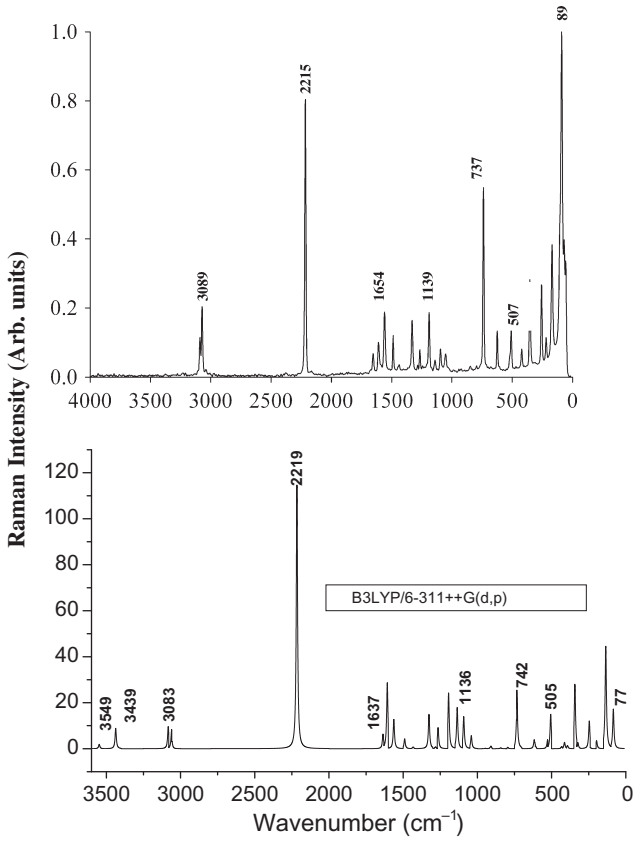

Fig. 3. Comparison of experimental (top) and theoretical (bottom) FT-Raman spectrum of 2-amino-4-chlorobenzonitrile.

simpler molecules global scaling (or uniform scaling) of the theoretical force field with one common scale factor may prove satisfactory [25]. It has been shown, however, that application of multiple scale factors, i.e. selective scaling of the ab initio calculated force field developed by Pulay et al. [26,27,18], leads to better results. The natural coordinates are constructed, which were defined as proposed by Pulay et al. [26,29]. Following the SQMFF procedure [18,27–29], the harmonic force field was scaled using the recommended scaling factors of Rauhut and Pulay [18,27].

5.2.1. C—H vibrations

The hetero aromatic structure shows the presence of C—H stretching vibrations in the region 3100–3000 cm^{-1} which is the characteristic region for the ready identification of C—H stretching vibrations [30]. In this region, the bands are not affected appreciably by the nature of substituents. The C—H stretching modes usually appear with strong Raman intensity and are highly polarized. May be owing to this high polarization, Raman bands have not been observed in experimental spectra. In the FT-IR spectrum, the band at 3087 cm^{-1} is assigned to the C—H stretching vibrations. In the FT-Raman spectrum, the bands observed at 3070 and 3089 cm^{-1} are attributed to C—H stretching vibrations. The vibrations assigned to aromatic C—H stretch in the region 3060–3085 cm^{-1} predicted theoretically at B3LYP/6-311++G(d,p) are in good agreement with the experimental assignment 3055–3085 cm^{-1} [15,31]. As indicated by the TED, these three modes (mode nos. 3–5) involve approximately 100% contribution suggesting that they are pure stretching modes.

The three in-plane C—H bending vibrations appear in the range 1300–1000 cm^{-1} in the substituted benzenes and the three out-of-plane bending vibrations occur in the frequency range 1000–750 cm^{-1} [15,32]. For our title molecule, the C—H in-plane bending vibrations are observed in the region 1097–1281 cm^{-1} in FT-IR and 1094–1265 cm^{-1} in FT-Raman. The frequencies calculated by DFT method in the range 1075–1261 cm^{-1} (mode nos. 13–17) are well correlated with the experimental frequencies and the maximum TED contribution is 80% C—H ipb. The C—H out-of-plane bending vibrations predicted theoretically at 943 and 794 cm^{-1} are coinciding very well with the observed frequencies at 936 and 786 cm^{-1}, respectively.

5.2.2. C—C and C—C—C vibrations

In benzonitriles, the distance between two carbon atoms changes the ring angles because of its substituents groups such as cyanogens. There are six equivalent C—C bonds in benzene and consequently there will be six C—C stretching vibrations. The bands are observed at 1435, 1565, 1609 and 1642 cm^{-1} in FT-IR are identified as C—C stretching vibrations. The ring breathing mode is assigned at 715 cm^{-1} in FT-IR. The theoretically computed value at 736 cm^{-1} coincides well with experimental observation. The theoretically scaled C—C stretching vibrations by DFT method are at 1411, 1539, 1582 and 1590 cm^{-1} shows excellent agreement with recorded FT-IR spectral data. The theoretically calculated C—C—C in-plane and out-of-plane bending modes have been found to be consistent with the recorded spectral values.

5.2.3. C—N and C≡N vibrations

The geometry of the cyano group (C—N) is affected insignificantly by the substitution of Cl and NH_2 on the phenyl ring. Hence

the vibrational wavenumber on the cyano group remains almost unchanged from the benzonitrile molecule. For the aromatic compound which bears a C—N group attached to the ring, a band of good intensity has been absorbed in the region 2240–2221 cm^{-1} [33] and it is being attributed to C—N stretching. In the case of 2-amino-5-chlorobenzonitrile the strong FT-IR band at 2230 cm^{-1} was assigned to C≡N stretching vibration [15]. For 2A4CBN, the C≡N stretching mode appears in our calculation at 2213 cm^{-1} (FT-IR), 2215 cm^{-1} (FT-Raman) with a composition of νC≡N 90%, νC—C 10%. The C—C≡N stretching vibration is observed at 1186 cm^{-1} (FT-IR) and 1189 cm^{-1} (FT-Raman) and calculated by theoretically at 1184 cm^{-1} (mode no. 15). The TED of this vibration is 37% νC—C≡N, with minor contribution of 25% βC—C—C and 15% βC—H. The βC—C≡N bending vibrations are observed at lower frequencies.

5.2.4. NH_2 vibrations

The stretching, scissoring and rocking deformation of amino group appeared around 3500–3000, 1700–1600, 1150–900 cm^{-1} [34], respectively in IR absorption spectra. The NH_2 asymmetric and symmetric stretching vibrations are observed experimentally at 3456 and 3369 cm^{-1} and calculated theoretically by DFT/B3LYP at 3487 and 3378 cm^{-1} (mode nos. 1 and 2). These modes are pure modes as it is evident from TED calculations, it is contributing 100% of νNH_2. The NH_2 scissoring mode is observed at 1642 cm^{-1} (FT-IR) and 1654 cm^{-1} (FT-Raman). The scissoring mode is calculated theoretically at 1590 cm^{-1} and it shows a very good agreement with experimental data with TED contribution of 88%. The NH_2 rocking mode is predicted at 1012 cm^{-1} (mode no. 18) and experimentally observed at 1052 cm^{-1} and 1050 cm^{-1} in FT-IR and FT-Raman, respectively. The TED of this mode is 41% rNH_2 with 35% νC—C. The NH_2 wagging mode is calculated at 323 cm^{-1}.

5.2.5. C—Cl vibrations

The vibrations belonging to the bond between the ring and halogen atoms are worth to discuss here since mixing of vibrations are possible due to the lowering of molecular symmetry and the presence of heavy atoms on periphery of the molecule [35,36]. The X-sensitive C—Cl stretching band is expected around 1105–1045 cm^{-1} [37]. The —C—Cl stretching vibration in our title molecule is strongly coupled with in-plane bending vibrations of CCC and stretching vibrations of C—NH_2. As revealed by the TED, the —(C—Cl) vibration has the large contribution to the medium band observed at 919 cm^{-1} in the FT-IR spectrum (mode no. 19). The theoretically calculated value at 914 cm^{-1} by DFT method show very good correlation with our experimental observation. The scaled value of 615 cm^{-1} (mode no. 26) also involves large contribution of TED from the —(C—Cl) stretch. However our experimental observations do not show any such band in this region. For 2-amino-5-chlorobenzonitrile [15] molecule the strong FT-IR band at 900 cm^{-1} with 86% TED was assigned to C—Cl stretching mode.

5.3. NBO analysis

NBO analysis provides the most accurate possible 'natural Lewis structure' picture of ø, because all orbital details are mathematically chosen to include the highest possible percentage of the electron density. A useful aspect of the NBO method is that it gives information about interactions in both filled and virtual orbital spaces that could enhance the analysis of intra- and intermolecular interactions.

The second order Fock matrix was carried out to evaluate the donor–acceptor interactions in the NBO analysis [38]. The interactions result is a loss of occupancy from the localized NBO of the idealized Lewis structure into an empty non-Lewis orbital. For each

Table 3
NBO results showing formation of Lewis and non-Lewis orbitals for 2-amino-4-chlorobenzonitrile.

Bond (A—B)	Type	ED/energy (a.u)	ED_A (%)	ED_B (%)	NBO	s (%)	p (%)
C1—C2	σ	1.979	50.70	49.30	$0.7120(sp^{1.59})C + 0.7021(sp^{1.83})C$	38.58	61.38
		−0.749				35.37	64.59
C1—C2	σ^*	0.027	49.30	50.70	$0.7021(sp^{1.59})C—0.7120(sp^{1.83})C$	38.58	61.38
		0.536				35.37	64.59
C1—C6	σ	1.976	50.08	49.92	$0.7077(sp^{1.62})C + 0.7066(sp^{1.78})C$	38.16	61.79
		−0.750				36.02	63.94
C1—C6	σ^*	0.026	49.92	50.08	$0.7066(sp^{1.62})C—0.7120(sp^{1.78})C$	38.16	61.79
		−0.296				36.02	63.94
C3—C4	σ	1.968	48.24	51.76	$0.6945(sp^{1.83})C + 0.7195(sp^{1.69})C$	35.27	64.69
		−0.738				37.16	62.81
C3—C4	σ^*	0.019	51.76	48.24	$0.7195(sp^{1.83})C—0.6945(sp^{1.69})C$	35.27	64.69
		0.539				37.16	62.81
C4—C5	σ	1.969	50.50	49.50	$0.7106(sp^{1.76})C + 0.7036(sp^{1.74})C$	36.26	63.69
		−0.751				36.54	63.42
C4—C5	σ^*	0.027	49.50	50.50	$0.7036(sp^{1.83})C—0.7106(sp^{1.69})C$	36.26	63.69
		−0.291				36.54	63.42
C1—Cl10	σ	1.988	46.00	54.00	$0.6782(sp^{3.32})Cl + 0.7348(sp^{4.80})C$	23.12	76.68
		−0.735				17.16	82.34
C1—Cl10	σ^*	0.029	54.00	46.00	$0.7348(sp^{3.32})Cl—0.6782(sp^{4.80})C$	23.12	76.68
		0.119				17.16	82.34
C11—N12	σ	1.996	41.96	58.04	$0.6478(sp^{1.09})C + 0.7618(sp^{1.09})N$	47.91	52.07
		−1.083				47.69	51.91
C11—N12	σ^*	0.007	58.04	41.96	$0.7618(sp^{1.09})C—0.6478(sp^{1.09})N$	47.91	52.07
		0.924				47.69	51.91
C5—N13	σ	1.990	40.92	59.08	$0.6397(sp^{2.81})C + 0.7686(sp^{1.75})N$	26.25	73.66
		−0.773				36.40	63.56
C5—N13	σ^*	0.019	59.08	40.92	$0.7686(sp^{2.81})C —0.6397(sp^{1.75})N$	26.25	73.66
		0.316				36.40	63.56
Cl10	LP(1)	1.991	–	–	$sp^{0.21}$	82.96	17.03
		−0.954					
N12	LP(1)	1.969	–	–	$sp^{0.91}$	52.40	47.51
		−0.524					
N13	LP(1)	1.834	–	–	$sp^{1.00}$	0.00	100.0
		−0.274					

Table 4
Second order perturbation theory analysis of Fock matrix in NBO basis for 2-amino-4-chlorobenzonitrile.

Donor (i)	Type	ED/e	Acceptor (j)	Type	ED/e	$E^{(2)}$[a] (KJ mol^{-1})	$E(j)$–$E(i)$[b] (a.u)	$F(i,j)$[c] (a.u)
C1—C2	σ	1.979	C1—C6	σ^*	0.026	3.35	1.28	0.059
			C2—C3	σ^*	0.014	2.89	1.30	0.055
C1—C6	σ	1.976	C1—C2	σ^*	0.027	3.33	1.29	0.059
			C5—C6	σ^*	0.019	3.29	1.29	0.058
			C5—N13	σ^*	0.019	3.78	1.07	0.057
C1—C6	π	1.705	C2—C3	π^*	0.322	16.15	0.30	0.062
			C4—C5	π^*	0.448	22.03	0.29	0.074
C2—C3	σ	1.967	C1—C2	σ^*	0.027	3.46	1.26	0.059
			C1—Cl10	σ^*	0.029	4.87	0.85	0.057
			C4—Cl11	σ^*	0.034	4.06	1.07	0.059
	π	1.678	C1—C6	π^*	0.390	23.47	0.27	0.072
			C4—C5	π^*	0.448	16.10	0.28	0.061
C4—C5	σ	1.969	C3—C4	σ^*	0.019	4.41	1.29	0.067
			C5—C6	σ^*	0.019	3.60	1.29	0.061
	π	1.639	C1—C6	π^*	0.390	16.49	0.28	0.061
			C2—C3	π^*	0.322	23.69	0.29	0.075
			C11—N12	π^*	0.008	12.34	0.38	0.067
C4—C11	σ	1.981	C11—N12	σ^*	0.007	4.58	1.61	0.077
Cl10	LP(3)	1.921	C1—C6	π^*	0.390	13.49	0.32	0.064
N12	LP(1)	1.999	C4—C11	σ^*	0.034	10.57	0.86	0.085
N13	LP(1)	1.999	C4—C5	π^*	0.448	30.00	0.27	0.087
C1—C6	π^*	1.705	C2—C3	π^*	0.322	179.19	0.02	0.080
			C4—C5	π^*	0.448	384.30	0.01	0.086

[a] $E^{(2)}$ means energy of hyper conjugative interaction (stabilization energy).
[b] Energy difference between donor and acceptor i and j NBO orbitals.
[c] $F(i,j)$ is the Fock matrix element between i and j NBO orbitals.

Table 5
Theoretical electronic absorption spectra values of 2-amino-4-chlorobenzonitrile.

TD-DFT/B3LYP/6-311++G(d,p)								
Gas			DMSO			$CDCl_3$		
Wave lengths λ (nm)	Excitation energies (eV)	Oscillator strengths (f)	Wave lengths λ (nm)	Excitation energies (eV)	Oscillator strengths (f)	Wave lengths λ (nm)	Excitation energies (eV)	Oscillator strengths (f)
293.80	4.2200 (38 → 41, 39 → 40)	0.0681	308.46	4.0195 (38 → 41, 39 → 40)	0.1007	304.70	4.0691 (38 → 41, 39 → 40)	0.0988
234.62	5.2844 (39 → 42)	0.0070	232.30	5.3373 (39 → 42)	0.0088	232.34	5.3364 (39 → 42, 39 → 44)	0.0084
225.66	5.4943 (39 → 43)	0.0006	226.97	5.4626 (39 → 43, 39 → 44)	0.0023	226.17	5.4818 (39 → 43)	0.0023

donor (i) and acceptor (j), the stabilization energy $E^{(2)}$ associated with the delocalization $i \rightarrow j$ is estimated as

$$E_2 = \Delta E_{ij} = q_i \frac{F(i,j)^2}{\varepsilon_j - \varepsilon_i}$$

where q_i is the donor orbital occupancy, are ε_i and ε_j diagonal elements and $F(i,j)$ is the off diagonal NBO Fock matrix element.

The natural bond orbital (NBO) calculation was performed using NBO 3.1 program implemented in the Gaussian 03 [16] package at the DFT/B3LYP level in order to understand various second-order interactions between the filled orbitals of one subsystem and vacant orbitals of another subsystem, which is a measure of the delocalization or hyperconjugation. The hyperconjugative interaction energy was deduced from the second-order perturbation approach [39]. Delocalization of electron density between occupied Lewis-type (bond or lone pair) NBO orbitals and formally unoccupied (antibond or Rydberg) non-Lewis NBO orbitals corresponds to a stabilizing donor–acceptor interaction. The corresponding results have been tabulated in Table 3. In NBO analysis large $E^{(2)}$ value shows the intensive interaction between electron-donors and electron-acceptors and greater the extent of conjugation of the whole system, the possible intensive interactions are given in Table 4. The second-order perturbation theory analysis of Fock matrix in NBO basis shows strong intramolecular hyperconjugative interactions of electrons.

The intramolecular interaction are formed by the orbital overlap between σ(C—C), σ^*(C—C), π(C—C), π^*(C—C) bond orbital which results intramolecular charge transfer (ICT) causing stabilization of the system. These interactions are observed as increase in electron density (ED) in C—C anti-bonding orbital that weakens the respective bonds. The electron density of conjugated bond of aromatic ring (~1.99e) clearly demonstrates strong delocalization.

The strong intramolecular hyper conjugation interaction of the σ and π electrons of C—C, C—H, C—N and C—Cl to the anti C—C,

Table 6
Calculated energy values of 2-amino-4-chlorobenzonitrile in its ground states with singlet symmetry and dipole moment at DFT method.

TD-DFT/B3LYP/6-311++G(d,p)			
Energy (a.u.)	Gas	DMSO	$CDCl_3$
HOMO	−0.24544	−0.23351	−0.23622
LUMO	−0.06542	−0.06014	−0.06096
HOMO–LUMO gap (ΔE)	−0.18002	−0.17337	−0.17526
HOMO − 1	−0.27918	−0.27303	−0.27414
LUMO + 1	−0.03753	−0.02722	−0.02944
HOMO–LUMO gap (ΔE)	−0.24165	−0.24581	−0.2447
Dipole moment, μ(D)	2.7170	3.5732	3.3407

C—H and C—N bond leads to stabilization of some part of the ring as evident from Table 3. The intramolecular hyperconjugative interaction of the σ(C1—C6) distribute to σ^*(C1—C2), (C5—C6), leads to less stabilization of 3.0 kJ/Mol. This enhanced further conjugate with anti-bonding orbital of π^* (C2—C3) and (C4—C5) which leads to strong delocalization of 16.15 and 22.03 kJ/Mol, respectively. The same trend is observed as in the entire part of the ring as shown in Table 4.

There occurs a strong intramolecular hyperconjugative interaction, from LP(3)Cl10 → π^*(C1—C6) and LP(1)N13 → π^*(C4—C5) which increases ED (1.921 and 1.999e) that weakens the respective bonds leading to stabilization of 13 and 30 kJ mol respectively.

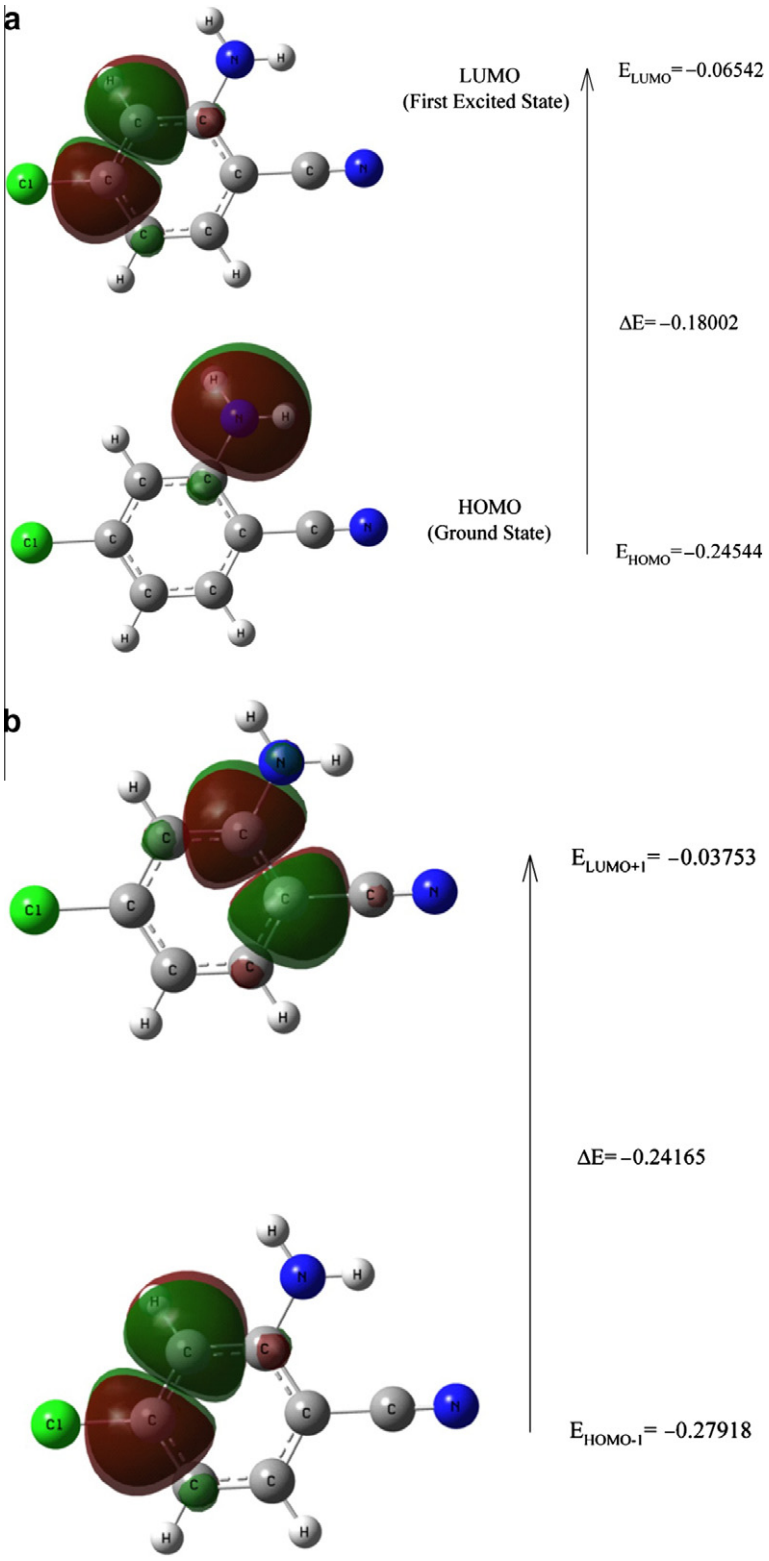

Fig. 4. (a and b) The atomic orbital compositions of the frontier molecular orbital for 2-amino-4-chlorobenzonitrile.

The increased electron density at the chlorine atoms leads to the elongation of C—Cl bond and a lowering of the C—Cl stretching wavenumber. The electron density (ED) is transferred from the n(Cl) to the anti-bonding σ^* orbital of the C—C bond, explaining both the elongation and the red shift. The C=N stretching mode can be used as a good probe for evaluating the bonding configuration around the cyanide N atom and the electronic distribution of the benzene molecule. The n–π conjugation between the cyanide nitrogen lone pair electrons and benzene ring system is strong in the ground state. The LP(1)(N12) → $n\sigma^*$(C4—C11) energies are 10.57 kJ mol respectively shows n-conjugation between N and benzene ring.

The NBO analysis also describes the bonding in terms of the natural hybrid orbital LP(1)N13, which occupy a higher energy orbital −0.274 a.u.) with considerable p-character (100%) and low occupation number (1.834 a.u.), and the other LP(1)N12 occupy an lower energy orbital (−0.524 a.u.) with s-character (52.40%) and occupation number (1.969 a.u.) with p-character (47.51%).

5.4. UV–VIS spectra analysis

Ultraviolet spectra analyses of 2-amino-4-chlorobenzonitrile have been investigated by theoretical calculation. Absorption maxima (λ_{max}) (nm) for lower-lying singlet states of the molecule have been calculated by TD-DFT/B3LYP method. The calculated visible absorption maxima of λ which are a function of the electron availability have been reported in Table 5. Calculations of the molecular orbital geometry show that the visible absorption maxima of this molecule correspond to the electron transition between frontier orbitals such as translation from HOMO to LUMO. As can be seen from the Table 5, the calculated absorption maxima values have been found to be 293.80, 234.62, 225.66 nm for gas phase, 308.46, 232.30, 226.97 nm for DMSO solution and 304.70, 232.34, 226.17 nm for $CDCl_3$ solution at DFT/B3LYP/6-311++G(d,p) method. As can be seen, calculations performed at DMSO and $CDCl_3$ are very close to each other when compared with gas phase. In addition, oscillator strength and excitation energies have also been depicted in Table 5.

5.5. HOMO–LUMO analysis

Highest occupied molecular orbital (HOMO) and lowest unoccupied molecular orbital (LUMO) are very important parameters for quantum chemistry. We can determine the way the molecule interacts with other species; hence, they are called the frontier orbitals. Both the highest occupied molecular orbital (HOMO) and lowest unoccupied molecular orbital (LUMO) are the main orbital take part in chemical stability. The HOMO represents the ability to donate an electron, LUMO as an electron acceptor represents the ability to obtain an electron. The HOMO and LUMO energy calculated by B3LYP/6-311++G(d,p) method is shown below. This electronic absorption corresponds to the transition from the ground to the first excited state and is mainly described by one electron excitation from the highest occupied molecular orbital (HOMO) to the lowest unoccupied molecular orbital (LUMO). Owing to the interaction between HOMO and LUMO orbital of a structure, transition state transition of π^*–π^* type is observed with regard to the molecular orbital theory [40]. Therefore, while the energy of the HOMO is directly related to the ionization potential, LUMO energy is directly related to the electron affinity. Energy difference between HOMO and LUMO orbital is called as energy gap that is an important stability for structures [41] and given in Table 6. In addition, 3D plots of highest occupied molecular orbitals (HOMOs) and lowest unoccupied molecular orbitals (LUMOs) are shown in Fig. 4a and 4b.

The HOMO is located over the amino group, the HOMO → LUMO transition implies an electron density transfer to ring from the amino group. Moreover, these orbital significantly overlap in their position for 2A4CBN. The atomic orbital compositions of the frontier molecular orbital are sketched in Fig. 4a and 4b.

HOMO energy (B3LYP) = −0.24544 a.u

LUMO energy (B3LYP) = −0.06542 a.u

HOMO—LUMO energy gap (B3LYP) = −0.18002-a.u

The calculated self-consistent field (SCF) energy of 2A4CBN is −839.56508 a.u. Moreover lower in the HOMO and LUMO energy gap explains the eventual charge transfer interactions taking place within the molecule.

6. Conclusion

The detailed interpretation of the vibrational spectra has been carried out with the aid of scaled quantum mechanical force field methodology. FT-IR and FT-Raman spectra of the 2-amino-4-chlorobenzonitrile have been recorded and analyzed. The molecular geometry, vibrational wavenumbers, NBO analysis, UV–Vis spectral analysis, HOMO and LUMO energy of 2-amino-4-chlorobenzonitrile in the ground state have been calculated by using density functional theory. The geometrical structure shows a little distortion due to the substitution of highly electronegative chlorine atom and nitrile group. The observed and the calculated wavenumbers are found to be in good agreement. The lowering of the HOMO–LUMO energy gap value has substantial influence on the intramolecular charge transfer and bioactivity of the molecule.

References

[1] B.S. Bahl, A. Bhal, Advanced Organic Chemistry, fourth ed., Springer, 1995. p. 1117.
[2] (a) K.A. Zachariasse, M. Grobys, T. Haar, Van der, A. Hebecker, Y.V. Ilichev, O. Morawski, I. Ruckert, W.J. Kuhnle, Photochem. Photobiol. A Chem. 105 (1997) 373;
(b) Y.V. Ilichev, W. Kuhnle, K.A. Zachariasse, J. Phys. Chem. 102 (1988) 5670.
[3] A. Kuwae, K. Machida, Spectrochim. Acta 35A (1979) 841.
[4] J.H.S. Green, D.J. Harrison, Spectrochim. Acta 32A (1976) 1279.
[5] S.P. Sinta, C.L. Chatterjee, Spectrosc. Lett. 9 (1976) 461.
[6] A.N. Pathak, B.K. Sinha, Indian J. Pure Appl. Phys. 18 (1980) 619.
[7] V.K. Rastogi, H.P. Mital, S.N. Sharma, S. Chattopadhya, Indian J. Phys. 65B (1991) 356.
[8] A.P. Kumar, G.R. Rao, Spectrochim. Acta 53A (1997). 2023, 2033, 2041, 2049.
[9] G. Bottura, S. Arora, J.K. Gupta, V.K. Rastogi, Asian J. Phys. 1 (1992) 58.
[10] R. Chandra, A. Singh, T.P. Singh, Asian J. Phys. 2 (1993) 50.
[11] V.K. Rastogi, C.B. Arora, S.K. Singhal, D.N. Singh, R.A. Yadav, Spectrochim. Acta 53A (1997) 2505.
[12] S. Mohan, R. Murugan, S. Srinivasan, Proc. Natl. Acad. Sci. India 62A (1992).
[13] V.K. Rastogi, M.A. Palafox, R.P. Tanwar, L. Mittal, Spectrochim. Acta 58A (2002) 1987.
[14] P.R. Varadwaj, A.I. Jaman, Z. Kisiel, L. Pszczółkowski, J. Mol. Spectrosc. 239 (2006) 88.
[15] V. Krishnakumar, S. Dheivamalar, Spectrochim. Acta 71A (2008) 465.
[16] Gaussian Inc., Gaussian 03 Program, Gaussian Inc., Wallingford, 2004.
[17] H.B. Schlegel, J. Comput. Chem. 3 (1982) 214.
[18] J. Baker, A.A. Jarzecki, P. Pulay, J. Phys. Chem. 102A (1998) 1412.
[19] P. Pulay, J. Baker, K. Wolinski, Chem. Phys. Lett. 358 (2002) 354.
[20] E.D. Glendening, A.E. Reed, J.E. Carpenter, F. Weinhold, NBO Version 3.1, TCI, University of Wisconsin, Madison, 1998.
[21] G. Keresztury, S. Holly, J. Varga, G. Besenyei, A.Y. Wang, J.R. Durig, Spectrochim. Acta 9A (1993) 2007.
[22] G. Keresztury, in: J.M. Chalmers, P.R. Griffith (Eds.), Raman Spectroscopy: Theory, Hand book of Vibrational Spectroscopy, vol. 1, John Wiley & Sons Ltd., New York, 2002.
[23] V.K. Rastogi, M.A. Palafox, S. Singhal, S.P. Ojha, W. Kiefer, Int. J. Quamtum Chem. 107 (2007) 1099.
[24] D. Britton, W.E. Noland, M.J. Pinnow, Acta Cryst. B56 (2000) 822.
[25] A.P. Scott, L. Radom, J. Phys. Chem. 100 (1996) 16502.
[26] P. Pulay, G. Fogarasi, G. Pongor, J.E. Boggs, A. Vargha, J. Am. Chem. Soc. 105 (1983) 7037.
[27] G. Rauhut, P. Pulay, J. Phys. Chem. 99 (1995) 3093.
[28] P. Pulay, G. Fogarasi, F. Pang, E. Boggs, J. Am. Chem. Soc. 101 (1979) 2550.

[29] F. Kalincsak, G. Pongor, Spectrochim. Acta 58A (2002) 999.
[30] G. Varsanyi, Assignment for Vibrational Spectra of Seven Hundred Benzene Derivatives, vols. 1–2, Academic Kiaclo, Budapest, 1973.
[31] V.K. Rastogi, M.A. Palafox, R.P. Tanwar, L. Mittal, Spectrochim. Acta 58A (2002) 1989.
[32] M. Silverstein, G. Clayton Basseler, C. Morill, Spectrometric Identification of Organic Compounds, Wiley, New York, 1981.
[33] R. Aquel, P.K. Verma, Indian J. Pure Appl. Phys. 20 (1982) 672.
[34] G. Socrates, Infrared and Raman Characteristic Group Frequencies – Tables and Charts, third ed., Wiley, Chichester, 2001.
[35] C. Lee, W. Yang, R.G. Parr, Phys. Rev. 37B (1988) 785.
[36] B. Lakshmaiah, G. Ramana Rao, J. Raman Spectrosc. 20 (1989) 439.
[37] N.B. Colthup, L.H. Daly, S.E. Wiberly, Introduction to Infrared and Raman Spectroscopy, third ed., Academic Press, Boston, 1990.
[38] A.E. Reed, L.A. Curtiss, F. Weinhold, Chem. Rev. 88 (1988) 899.
[39] J. Choo, S. Kim, H . Joo, Y. Kwon, J. Mol. Struct. (Theochem.) 587 (2002) 1.
[40] K. Fukui, Theory of Orientation and Stereoselection, Springer-Verlag, Berlin, 1975, see also: Fukui, K. Science 218 (1987) 747.
[41] D.F.V. Lewis, C. Ioannides, D.V. Parke, Xenobiotica 24 (1994) 401.